Restoring Ergodicity in a Strongly Disordered Interacting Chain

B. Krajewski,[1] L. Vidmar,[2,3] J. Bonča,[3,2] and M. Mierzejewski[1]
[1]Department of Theoretical Physics, Faculty of Fundamental Problems of Technology, Wrocław University of Science and Technology, 50-370 Wrocław, Poland
[2]Department of Theoretical Physics, J. Stefan Institute, SI-1000 Ljubljana, Slovenia
[3]Department of Physics, Faculty of Mathematics and Physics, University of Ljubljana, SI-1000 Ljubljana, Slovenia

(Received 13 September 2022; accepted 6 December 2022; published 20 December 2022)

We consider a chain of interacting fermions with random disorder that was intensively studied in the context of many-body localization. We show that only a small fraction of the two-body interaction represents a true local perturbation to the Anderson insulator. While this true perturbation is nonzero at any finite disorder strength W, it decreases with increasing W. This establishes a view that the strongly disordered system should be viewed as a weakly perturbed integrable model, i.e., a weakly perturbed Anderson insulator. As a consequence, the latter can hardly be distinguished from a strictly integrable system in finite-size calculations at large W. We then introduce a rescaled model in which the true perturbation is of the same order of magnitude as the other terms of the Hamiltonian, and show that the system remains ergodic at arbitrary large disorder.

DOI: 10.1103/PhysRevLett.129.260601

Introduction.—The interplay between disorder and interactions in quantum systems has recently attracted significant interest. Some of the most exciting ideas were formulated within the framework of many-body localization (MBL), which is conjectured to be as a phase of matter that violates ergodicity in spite of the presence of interactions [1–7].

The disordered systems exhibit several unusual properties, in particular extremely slow dynamics [8–15] that was frequently interpreted as a precursor to MBL [16–23]. However, one of the most important questions about MBL is related to its stability in the thermodynamic limit. Until recently, the results of essentially all studies in one-dimensional (1D) spin-1/2 systems with disorder were interpreted in terms of a stable MBL phase [8–12,24–48]. Recent work has, however, highlighted robustness of ergodicity at moderate disorder [49], which may eventually suggest that the stability of MBL may not be taken for granted. Signatures of robustness of ergodicity were also reported in several subsequent works [14,15,50–54], and they triggered, among others, activities to gain a better insight into the avalanche theory of ergodicity breaking transitions [55–62]. However, many recent numerical studies are interpreted in terms of the existence of a stable MBL phase [60,63–80]. Then, the MBL-to-thermal phase transition may occur at much stronger disorders than suggested by earlier numerical calculations [60].

Motivated by these open questions, it is an outstanding problem to understand why exact numerical studies can give rise to the formulation of contradictory expectations for the same models in the thermodynamic limit. More generally, what are the crucial ingredients of interacting systems with disorder that make identification of their key physical properties so challenging?

This Letter provides new perspective into studies of robustness of ergodicity and its detection in finite systems. For the model of interacting spinless fermions with disorder, which is mappable onto the paradigmatic random-field Heisenberg chain, we show that only a small fraction of the two-body interaction represents a true local perturbation to the Anderson insulator. The true perturbation becomes smaller with increasing disorder. Eventually, the true perturbation becomes too weak at very strong disorder to be captured by finite-size numerical calculations. Consequently, the strongly disordered system should be viewed as a weakly perturbed Anderson insulator. As an application of this insight, we introduce a rescaled model in which the strength of the true perturbation matches the energy density of the Anderson insulator. We argue that the latter model remains ergodic at essentially any finite disorder, and show that the matrix elements of observables are consistent with the eigenstate thermalization hypothesis (ETH) [81–84].

Setup.—We study interacting fermions in a 1D disordered lattice with L sites and periodic boundary conditions. The system is described by the Hamiltonian $H = H_0 + H_\Delta$, referred to as the *standard model* further on. The first term describes the Anderson insulator,

$$H_0 = \sum_{i=1}^{L} h_i,$$
$$h_i = \frac{1}{2}(a_{i+1}^\dagger a_i + \text{H.c.}) + \frac{\epsilon_i}{2}\left(n_i - \frac{1}{2}\right) + \frac{\epsilon_{i+1}}{2}\left(n_{i+1} - \frac{1}{2}\right), \quad (1)$$

where ϵ_i is a random potential with box distribution, $-W \le \epsilon_i \le W$, $a_i^\dagger$ creates a spinless fermion at site i, and $n_i = a_i^\dagger a_i$. The second term is the two-body interaction,

$$H_\Delta = \Delta \sum_{i=1}^{L} N_i, \qquad N_i = \left(n_i - \frac{1}{2}\right)\left(n_{i+1} - \frac{1}{2}\right), \quad (2)$$

where we take $\Delta = 1$ so that H can be mapped onto to the widely studied random-field Heisenberg model. The noninteracting part (i.e., the integrable part) of the Hamiltonian is diagonal in the Anderson basis

$$H_0 = \sum_\alpha \varepsilon_\alpha Q_\alpha + \text{const}, \qquad Q_\alpha = 2a_\alpha^\dagger a_\alpha - 1, \quad (3)$$

where $a_\alpha = \sum_i u_{i\alpha}^* a_i$ and $u_{i\alpha} = \langle i|\alpha\rangle$ are components of the single-particle wave function of the Anderson state α.

As a central step of our approach, we split the interaction term in Eq. (2) into two orthogonal parts,

$$H_\Delta = H_\Delta^{\parallel} + H_\Delta^{\perp}, \quad \text{with} \quad \langle H_\Delta^{\parallel} H_\Delta^{\perp}\rangle = 0, \quad (4)$$

where orthogonality is defined via the Hilbert-Schmidt inner product as $\langle AB\rangle = (1/Z)\mathrm{Tr}(A^\dagger B)$, the trace is carried out over many-body states, and Z is the dimension of the Fock space. In Eq. (4), $H_\Delta^{\parallel}$ represents a projection of H_Δ onto local integrals of motion of the Anderson insulator; thus $[H_\Delta^{\parallel}, H_0] = 0$. As a consequence, we identify the interaction in $H_\Delta^{\perp}$ as a *true perturbation* to the Anderson insulator, and we argue that it represents a local Hamiltonian. The idea of our approach is sketched in Fig. 1(a). Here, locality of operators (e.g., h_i or N_i) refers to the size of their support in real space which is fixed and does not grow with L. Linear combinations of the latter operators (e.g., H_0 or H_Δ) are also considered as local.

Below we show that the squared norm of the true perturbation $\|H_\Delta^{\perp}\|^2$ decays asymptotically for large W as $1/W^2$, whereas the squared norm of the Anderson model $\|H_0\|^2$ grows as W^2. Then, for sufficiently large W, the perturbation appears to be too weak to break integrability of a finite system. Here, the squared norms of observables are defined as $\|A\|^2 = \langle AA\rangle$.

Local integrals of motion.—The traceless operators Q_α from Eq. (3) represent the one-body local integrals of motion of the Anderson insulator. We briefly refer to them as LIOMs. We sort them according to the maxima of the single-particle wave functions $u_{i\alpha}$, i.e., we find $i_\alpha = \max_i |u_{i\alpha}|$ and sort them such that $i_\alpha \le i_{\alpha'}$ for $\alpha \le \alpha'$. Roughly speaking, for open boundary conditions the Anderson states with $\alpha \ll L$ are localized at the left edge of the system whereas the states with $\alpha \sim L$ are localized at the right edge. Importantly, a remarkable property of the Anderson insulator is that not only the LIOMs Q_α are local,

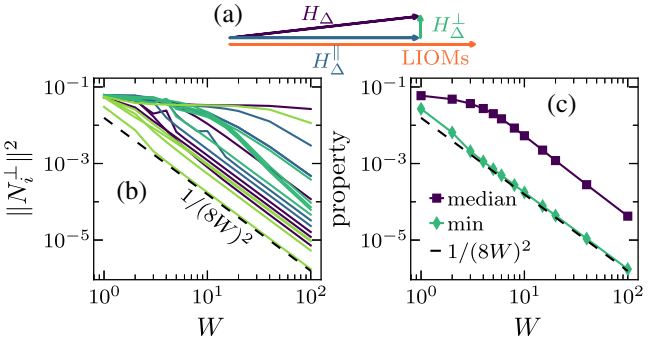

FIG. 1. (a) Sketch of the construction in Eq. (4). (b) Dependence of $\|N_i^{\perp}\|^2$ on W, where various curves of the same color correspond to different i but the same disorder realization [we keep $\epsilon_i/W = \text{const}$ when increasing W]. Various colors correspond to different realizations of disorder. (c) Two statistical properties of $\|N_i^{\perp}\|^2$ from 10^4 curves as those in (b): median and minimum. Dashed line is the lower bound $1/(8W)^2$; see the Supplemental Material [85]. The results in (b),(c) are obtained at $L = 14$ and $L/2$ fermions.

but so also are their products, $Q^{(2)}_{\alpha,d} \equiv Q_\alpha Q_{\alpha+d}$, provided that the distance $d = 1, \ldots, d_{\max}$ is small compared with L and $d_{\max}$ does not grow with the system size [86]. We briefly refer to these $Q^{(2)}_{\alpha,d}$ as two-body LIOMs.

It is straightforward to show that H_Δ from Eq. (2) has no projection on traceless LIOMs Q_α; see the Supplemental Material [85] for details. Therefore, we introduce an operator $N_i^{\parallel}$ that is a linear combination of two-body LIOMs, such that

$$N_i^{\parallel} = \sum_{d=1}^{d_{\max}} \sum_{\alpha=1}^{L} \langle Q^{(2)}_{\alpha,d} N_i\rangle Q^{(2)}_{\alpha,d}, \qquad N_i^{\perp} = N_i - N_i^{\parallel}. \quad (5)$$

The operator $N_i^{\parallel}$ can be interpreted as a projection of a local interaction onto two-body LIOMs, and hence it corresponds to an interaction that does not break integrability of the Anderson insulator. In contrast, $N_i^{\perp}$ can be viewed as the true perturbation.

We stress two important technical details. First, we only consider results for $d_{\max} = 2$ in this Letter, whereas in the Supplemental Material [85] we show that additional contributions coming from $d_{\max} > 2$ are negligible at strong disorder. Second, in the Fock space that consists of 2^L many-body configurations, the occupations of LIOMs Q_α are independent and their products $Q^{(2)}_{\alpha,d}$ are mutually orthogonal and normalized, i.e., $\langle Q^{(2)}_{\alpha,d} Q^{(2)}_{\alpha',d'}\rangle = \delta_{\alpha,\alpha'}\delta_{d,d'}$. As a consequence, Eq. (5) represents an orthogonal projection for which $\langle N_i^{\parallel} N_i^{\perp}\rangle = 0$. However, the actual calculations are carried out in a subspace with $L/2$ fermions, in which the LIOMs are not independent since $\sum_\alpha Q_\alpha = 0$, and their products are not traceless since

$\langle Q^{(2)}_{\alpha,d}\rangle = O(1/L)$. Then, one needs to reorthogonalize the set of $Q^{(2)}_{\alpha,d}$, as explained in the Supplemental Material [85].

Norm of the true perturbation.—We can now express $H^{\parallel}_{\Delta}$ and $H^{\perp}_{\Delta}$ from Eq. (4) using Eq. (5) as

$$H^{\parallel}_{\Delta} = \Delta \sum_{i=1}^{L} N^{\parallel}_i \quad \text{and} \quad H^{\perp}_{\Delta} = \Delta \sum_{i=1}^{L} N^{\perp}_i. \tag{6}$$

Since Eq. (5) assures locality of $N^{\parallel}_i$ and $N^{\perp}_i$, then $H^{\parallel}_{\Delta}$ and $H^{\perp}_{\Delta}$ are also local as they are defined as linear combinations of local operators N_i and $Q^{(2)}_{\alpha,d}$. The physical meaning of $H^{\perp}_{\Delta}$ can be understood by inspecting the identity (see the Supplemental Material [85] for a derivation)

$$\|H^{\perp}_{\Delta}\|^2 = \|H_{\Delta}\|^2 - \sum_{\alpha,d} \langle H_{\Delta} Q^{(2)}_{\alpha,d}\rangle^2, \tag{7}$$

which shows that the more two-body LIOMs $Q^{(2)}_{\alpha,d}$ one takes, the smaller is the norm of $H^{\perp}_{\Delta}$. Indeed, the essence of our approach is a systematic elimination of local contributions to H_{Δ} which commute with the integrable Hamiltonian H_0.

Figures 1(b) and 1(c) study the dependence on W of the squared norms $\|N^{\perp}_i\|^2$ that contribute to the norm of $H^{\perp}_{\Delta}$ in Eq. (6). Each curve in Fig. 1(b) is obtained for a single site i and a single realization of disorder, while Fig. 1(c) shows the median and the minimum of 10^4 curves as those in Fig. 1(b). One observes huge fluctuations between various sites and disorder realizations. Nevertheless, at sufficiently large W all curves eventually decay as $\|N^{\perp}_i\|^2 \propto 1/W^2$; see Fig. 1(b). For strong disorder we establish an L-independent bound $\|N^{\perp}_i\|^2 \geq 1/(8W)^2$, which accurately reproduces the numerical results in Fig. 1(c) already at $W > 3$. The derivation of the bound and the L dependence of $\|N^{\perp}_i\|^2$ are discussed in the Supplemental Material [85].

Summarizing this part, we stress that the perturbation to the Anderson insulator is not determined by the entire interaction term but rather by the projected operators $N^{\perp}_i$. This perturbation becomes very weak at strong disorder, $\|N^{\perp}_i\| \sim 1/W$, but remains nonzero for arbitrary finite W. Obviously, such a small but nonvanishing perturbation poses a challenge for finite-size numerical calculations.

Ergodicity in the rescaled model.—We complement the above analysis by introducing a model in which the norm of the true perturbation does not vanish with increasing W. To this end we study the *rescaled model* Hamiltonian

$$\tilde{H} = \sum_i h_i + \sum_i \frac{\|h_i\|}{\|N^{\perp}_i\|} N^{\perp}_i, \tag{8}$$

where h_i denotes the local term (the energy density operator) of the Anderson model from Eq. (1) and $N^{\perp}_i$ represents the density of the true perturbation from Eq. (6). Both energy density operators h_i and N_i are defined on the link between sites i and $i+1$.

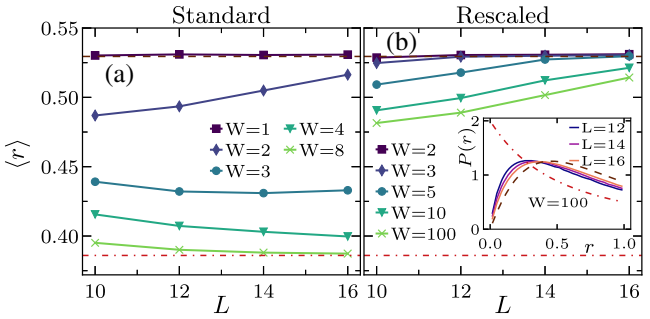

FIG. 2. Average gap ratio $\langle r\rangle$ at various L and W calculated in subspaces with $L/2$ fermions for (a) the standard model H from Eqs. (1) and (2), and (b) the rescaled model $\tilde{H}$ from Eq. (8). The averaging is carried out over $Z/3$ levels from the middle of the spectrum and over 4000 realizations of disorder. Inset in (b): probability density function $P(r)$ in the rescaled model at $W = 100$ and various L. Dash-dotted and dashed lines show the analytical predictions for the Poisson distribution [3] and the GOE [87,88], respectively (see also the Supplemental Material [85]).

The rescaled model [Eq. (8)] associates the strength of the perturbation with the strength of the disorder. In particular, the energy density of the true perturbation, cf. the second term on the rhs of Eq. (8), equals to the energy density of the Anderson insulator, for which the squared norm is $\|h_i\|^2 = (2 + \epsilon_i^2 + \epsilon_{i+1}^2)/16$. In the standard model, this roughly corresponds to the regime $\Delta \propto W$, for which one may expect an ergodic-to-nonergodic transition. (The nonergodic phase is conjectured to be reentrant as a function of the interaction strength; see, e.g., Fig. 1 in Ref. [12].) Below we explore robustness of ergodicity in the rescaled model [Eq. (8)].

As a simple test of ergodicity we study the average ratio of nearest level spacings $\langle r\rangle$ (i.e., the gap ratio); see the Supplemental Material [85] for a definition. The results are shown in Fig. 2(a) for the standard model H from Eqs. (1) and (2) and in Fig. 2(b) for the rescaled model $\tilde{H}$ from Eq. (8). In the standard model the results clearly deviate from the value $r \simeq 0.53$ in the Gaussian orthogonal ensemble (GOE) already at $W \gtrsim 3$, which was observed in many previous studies; see, e.g., Ref. [29]. However, the rescaled model remains ergodic at essentially all disorders, provided that the system is sufficiently large. As an additional test, we determine a distribution of r without any averaging, i.e., via collecting results from different disorder realizations as well as different eigenstates (from the middle third of the spectra). The inset of Fig. 2(b) shows the resulting probability density function $P(r)$ at various L. A comparison with analytical results [3,85,87–89] confirms that at large L the results approach the GOE prediction even at $W = 100$.

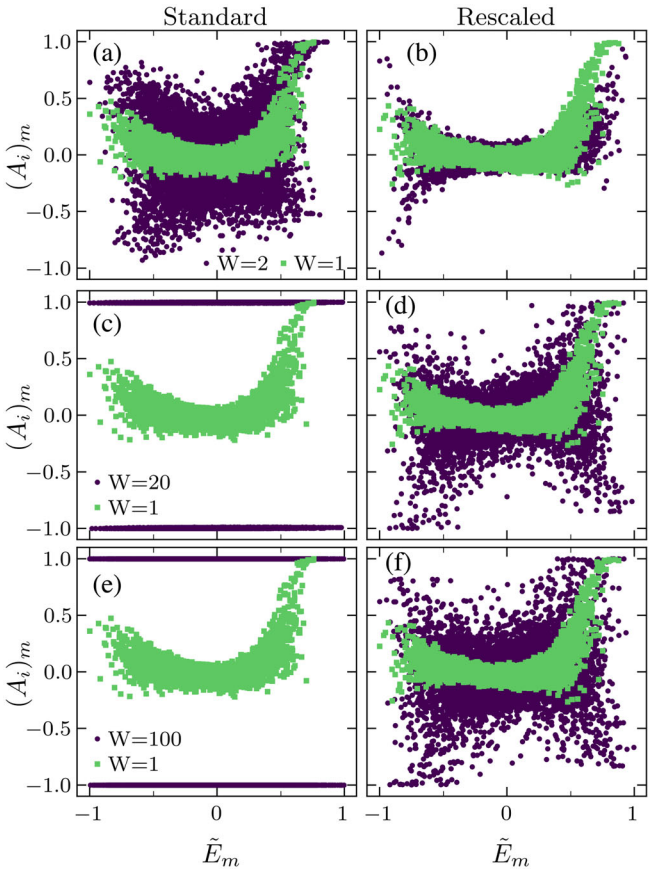

FIG. 3. Diagonal matrix elements $(A_i)_m = \langle E_m|A_i|E_m\rangle$, where $A_i = 2n_i - 1$, at $L = 16$ and different W. Results are shown for a single site i and a single realization of disorder. (a), (c), and (e) The standard model H from Eqs. (1) and (2). (b), (d), and (f) The rescaled model $\tilde{H}$ from Eq. (8). We rescale the energies as $\tilde{E}_m = E_m/|E_0|$, where E_0 is the ground state energy.

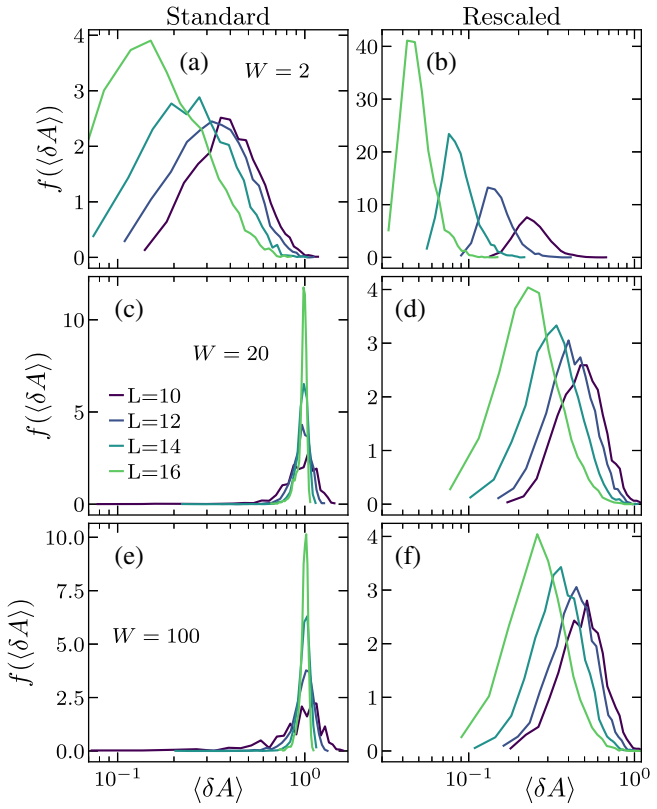

FIG. 4. Probability density function f of the eigenstate-to-eigenstate fluctuations $\langle\delta A\rangle$ from Eq. (9) for various L. The distributions are calculated at single lattice site and different realizations of disorder for (a), (c), (e) the standard model H and (b), (d), (f) the rescaled model $\tilde{H}$.

ETH analysis.—Finally, we test ergodicity of the rescaled Hamiltonian by studying the ETH. As observables we consider site occupations $A_i = 2n_i - 1$. Note that a linear combination of A_i, the imbalance $I = \sum_i (-1)^i A_i$, has been commonly studied in the context of ergodic-nonergodic transition and is accessible in cold-atom experiments [90]. Following a standard procedure [83], we calculate the diagonal matrix elements $(A_i)_m = \langle E_m|A_i|E_m\rangle$ where $|E_m\rangle$ are the many-body eigenstates of either the standard Hamiltonian H, or the rescaled Hamiltonian $\tilde{H}$; see Fig. 3. In a finite system described by the standard model, one observes $(A_i)_m = \pm 1$ at all energies at strong disorder [see Figs. 3(c) and 3(e)], and hence the ETH appears to be violated, suggesting nonergodic behavior. However, in the rescaled model the fluctuations of matrix elements are rather modest even at extremely strong disorder $W = 100$; see Fig. 3(f).

To study fluctuations of the diagonal matrix elements we calculate the average eigenstate-to-eigenstate fluctuations [91–93],

$$\langle\delta A\rangle = 1/\mathcal{Z}\sum_m |(A_i)_{m+1} - (A_i)_m|, \tag{9}$$

where the averaging is carried out over $\mathcal{Z} = Z/5$ states from the middle of the many-body spectrum. Figure 4 shows the probability density functions, $f(\langle\delta A\rangle)$, calculated at a single lattice site and different disorder realizations, for both the standard and the rescaled model. In the standard model one obtains $\langle\delta A\rangle \simeq 1$ at large disorder [cf. Figs. 4(c) and 4(e)], and the absence of any visible L dependence of the distributions may be interpreted as a violation of the ETH. In the rescaled model the distribution of $\langle\delta A\rangle$ is rather broad for the accessible system sizes. Nevertheless $\langle\delta A\rangle$ appears to decay with L suggesting $\langle\delta A\rangle \to 0$ in the thermodynamic limit. Because of the width of the distributions, one cannot unambiguously confirm exponential decay of the latter quantity. However, such a decay is strongly suggested by the decay of the median; see also the Supplemental Material [85].

Conclusions.—The main goal of this Letter was to identify the origin of complexity that emerges in the numerical studies of ergodicity in interacting fermions subject to random disorder. We showed that the two-body

interaction term H_Δ [Eq. (2)] cannot be considered as a perturbation to the Anderson insulator H_0 [Eq. (1)] since only a small fraction of the two-body interaction, denoted as $H_\Delta^\perp$, does not commute with H_0. We referred to the latter as the true local perturbation, and we showed that its relative norm decays with disorder as $\|H_\Delta^\perp\|/\|H_0\| \sim W^{-2}$. On the other hand, the norm is also bounded from below, so it remains nonzero at large but finite W. It is then clear that the interpretation of finite-size numerical calculations at large W is challenging since finite integrable systems with small perturbations are hardly distinguishable from strictly integrable systems.

It appears that the two regimes in which interpretation of numerical results has rather low ambiguity are the regime of small and moderate W, for which robustness of ergodicity was already established, and the regime where the strength of the true local perturbation $H_\Delta^\perp$ is rescaled. Here we considered the latter scenario and introduced a rescaled model in which the energy density of the perturbation equals that of the Anderson insulator. Studying the short-range level statistics and the ETH indicators in the rescaled model we showed that ergodicity persists up to extremely strong disorders, such as $W = 100$.

While focusing on 1D interacting fermions with random disorder, the main idea of our approach can be applied to an arbitrary model in any dimension. In particular, the method of identifying the true local perturbation allows for an unambiguous classification of the perturbation strength, and hence provides a new perspective into distinction between weakly and strongly perturbed integrable systems. Systems of broad interest to which the method can straightforwardly be applied in the near future are interacting fermions subject to quasiperiodic [94] or linear [95,96] potentials.

We acknowledge discussions with M. Rigol. We acknowledge support by the National Science Centre, Poland, via Project No. 2020/37/B/ST3/00020 (B. K and M. M.), the support by the Slovenian Research Agency (ARRS), Research Core Fundings Grants No. P1-0044 (L. V. and J. B.) and No. J1-1696 (L. V.).

[1] D. Basko, I. Aleiner, and B. Altshuler, Metal–insulator transition in a weakly interacting many-electron system with localized single-particle states, Ann. Phys. (Amsterdam) **321**, 1126 (2006).
[2] I. V. Gornyi, A. D. Mirlin, and D. G. Polyakov, Interacting Electrons in Disordered Wires: Anderson Localization and Low-t Transport, Phys. Rev. Lett. **95**, 206603 (2005).
[3] V. Oganesyan and D. A. Huse, Localization of interacting fermions at high temperature, Phys. Rev. B **75**, 155111 (2007).
[4] R. Nandkishore and D. A. Huse, Many-body-localization and thermalization in quantum statistical mechanics, Annu. Rev. Condens. Matter Phys. **6**, 15 (2015).
[5] E. Altman and R. Vosk, Universal dynamics and renormalization in many-body-localized systems, Annu. Rev. Condens. Matter Phys. **6**, 383 (2015).
[6] F. Alet and N. Laflorencie, Many-body localization: An introduction and selected topics, C. R. Phys. **19**, 498 (2018).
[7] D. A. Abanin, E. Altman, I. Bloch, and M. Serbyn, Colloquium: Many-body localization, thermalization, and entanglement, Rev. Mod. Phys. **91**, 021001 (2019).
[8] M. Žnidarič, T. Prosen, and P. Prelovšek, Many-body localization in the Heisenberg XXZ magnet in a random field, Phys. Rev. B **77**, 064426 (2008).
[9] M. Serbyn, Z. Papić, and D. A. Abanin, Universal Slow Growth of Entanglement in Interacting Strongly Disordered Systems, Phys. Rev. Lett. **110**, 260601 (2013).
[10] J. A. Kjäll, J. H. Bardarson, and F. Pollmann, Many-Body Localization in a Disordered Quantum Ising Chain, Phys. Rev. Lett. **113**, 107204 (2014).
[11] S. Bera, H. Schomerus, F. Heidrich-Meisner, and J. H. Bardarson, Many-Body Localization Characterized from a One-Particle Perspective, Phys. Rev. Lett. **115**, 046603 (2015).
[12] Y. Bar Lev, G. Cohen, and D. R. Reichman, Absence of Diffusion in an Interacting System of Spinless Fermions on a One-Dimensional Disordered Lattice, Phys. Rev. Lett. **114**, 100601 (2015).
[13] M. Serbyn, Z. Papić, and D. A. Abanin, Thouless energy and multifractality across the many-body localization transition, Phys. Rev. B **96**, 104201 (2017).
[14] D. Sels and A. Polkovnikov, Dynamical obstruction to localization in a disordered spin chain, Phys. Rev. E **104**, 054105 (2021).
[15] L. Vidmar, B. Krajewski, J. Bonča, and M. Mierzejewski, Phenomenology of Spectral Functions in Disordered Spin Chains at Infinite Temperature, Phys. Rev. Lett. **127**, 230603 (2021).
[16] D. J. Luitz and Y. Bar Lev, Anomalous Thermalization in Ergodic Systems, Phys. Rev. Lett. **117**, 170404 (2016).
[17] D. J. Luitz and Y. Bar Lev, The ergodic side of the many body localization transition, Ann. Phys. (Berlin) **529**, 1600350 (2017).
[18] M. Žnidarič, A. Scardicchio, and V. K. Varma, Diffusive and Subdiffusive Spin Transport in the Ergodic Phase of a Many-Body Localizable System, Phys. Rev. Lett. **117**, 040601 (2016).
[19] S. Gopalakrishnan, K. R. Islam, and M. Knap, Noise-Induced Subdiffusion in Strongly Localized Quantum Systems, Phys. Rev. Lett. **119**, 046601 (2017).
[20] M. Kozarzewski, P. Prelovšek, and M. Mierzejewski, Spin Subdiffusion in the Disordered Hubbard Chain, Phys. Rev. Lett. **120**, 246602 (2018).
[21] P. Prelovšek and J. Herbrych, Self-consistent approach to many-body localization and subdiffusion, Phys. Rev. B **96**, 035130 (2017).
[22] Y. B. Lev, D. M. Kennes, C. Klöckner, D. R. Reichman, and C. Karrasch, Transport in quasiperiodic interacting systems: From superdiffusion to subdiffusion, Europhys. Lett. **119**, 37003 (2017).
[23] P. Prelovšek, J. Bonča, and M. Mierzejewski, Transient and persistent particle subdiffusion in a disordered chain coupled to bosons, Phys. Rev. B **98**, 125119 (2018).

[24] A. Pal and D. A. Huse, Many-body localization phase transition, Phys. Rev. B **82**, 174411 (2010).
[25] C. Monthus and T. Garel, Many-body localization transition in a lattice model of interacting fermions: Statistics of renormalized hoppings in configuration space, Phys. Rev. B **81**, 134202 (2010).
[26] E. Khatami, M. Rigol, A. Relaño, and A. M. García-García, Quantum quenches in disordered systems: Approach to thermal equilibrium without a typical relaxation time, Phys. Rev. E **85**, 050102(R) (2012).
[27] J. H. Bardarson, F. Pollmann, and J. E. Moore, Unbounded Growth of Entanglement in Models of Many-Body Localization, Phys. Rev. Lett. **109**, 017202 (2012).
[28] A. De Luca and A. Scardicchio, Ergodicity breaking in a model showing many-body localization, Europhys. Lett. **101**, 37003 (2013).
[29] D. J. Luitz, N. Laflorencie, and F. Alet, Many-body localization edge in the random-field Heisenberg chain, Phys. Rev. B **91**, 081103(R) (2015).
[30] E. J. Torres-Herrera and L. F. Santos, Dynamics at the many-body localization transition, Phys. Rev. B **92**, 014208 (2015).
[31] M. Serbyn, Z. Papić, and D. A. Abanin, Criterion for Many-Body Localization-Delocalization Phase Transition, Phys. Rev. X **5**, 041047 (2015).
[32] T. Devakul and R. R. P. Singh, Early Breakdown of Area-Law Entanglement at the Many-Body Delocalization Transition, Phys. Rev. Lett. **115**, 187201 (2015).
[33] M. Serbyn and J. E. Moore, Spectral statistics across the many-body localization transition, Phys. Rev. B **93**, 041424(R) (2016).
[34] C. L. Bertrand and A. M. García-García, Anomalous Thouless energy and critical statistics on the metallic side of the many-body localization transition, Phys. Rev. B **94**, 144201 (2016).
[35] M. Mierzejewski, J. Herbrych, and P. Prelovšek, Universal dynamics of density correlations at the transition to the many-body localized state, Phys. Rev. B **94**, 224207 (2016).
[36] R. Steinigeweg, J. Herbrych, F. Pollmann, and W. Brenig, Typicality approach to the optical conductivity in thermal and many-body localized phases, Phys. Rev. B **94**, 180401(R) (2016).
[37] M. Filippone, P. W. Brouwer, J. Eisert, and F. von Oppen, Drude weight fluctuations in many-body localized systems, Phys. Rev. B **94**, 201112(R) (2016).
[38] V. Khemani, S. P. Lim, D. N. Sheng, and D. A. Huse, Critical Properties of the Many-Body Localization Transition, Phys. Rev. X **7**, 021013 (2017).
[39] V. Khemani, D. N. Sheng, and D. A. Huse, Two Universality Classes for the Many-Body Localization Transition, Phys. Rev. Lett. **119**, 075702 (2017).
[40] G. De Tomasi, S. Bera, J. H. Bardarson, and F. Pollmann, Quantum Mutual Information as a Probe for Many-Body Localization, Phys. Rev. Lett. **118**, 016804 (2017).
[41] F. Pietracaprina, G. Parisi, A. Mariano, S. Pascazio, and A. Scardicchio, Entanglement critical length at the many-body localization transition, J. Stat. Mech. (2017) 113102.
[42] J. Gray, S. Bose, and A. Bayat, Many-body localization transition: Schmidt gap, entanglement length, and scaling, Phys. Rev. B **97**, 201105(R) (2018).
[43] P. Sierant and J. Zakrzewski, Level statistics across the many-body localization transition, Phys. Rev. B **99**, 104205 (2019).
[44] M. Schiulaz, E. J. Torres-Herrera, and L. F. Santos, Thouless and relaxation time scales in many-body quantum systems, Phys. Rev. B **99**, 174313 (2019).
[45] N. Macé, F. Alet, and N. Laflorencie, Multifractal Scalings across the Many-Body Localization Transition, Phys. Rev. Lett. **123**, 180601 (2019).
[46] S. Roy, J. T. Chalker, and D. E. Logan, Percolation in Fock space as a proxy for many-body localization, Phys. Rev. B **99**, 104206 (2019).
[47] S. Roy and D. E. Logan, Fock-space correlations and the origins of many-body localization, Phys. Rev. B **101**, 134202 (2020).
[48] M. Tarzia, Many-body localization transition in Hilbert space, Phys. Rev. B **102**, 014208 (2020).
[49] J. Šuntajs, J. Bonča, T. Prosen, and L. Vidmar, Ergodicity breaking transition in finite disordered spin chains, Phys. Rev. B **102**, 064207 (2020).
[50] J. Šuntajs, J. Bonča, T. Prosen, and L. Vidmar, Quantum chaos challenges many-body localization, Phys. Rev. E **102**, 062144 (2020).
[51] M. Kiefer-Emmanouilidis, R. Unanyan, M. Fleischhauer, and J. Sirker, Evidence for Unbounded Growth of the Number Entropy in Many-Body Localized Phases, Phys. Rev. Lett. **124**, 243601 (2020).
[52] M. Kiefer-Emmanouilidis, R. Unanyan, M. Fleischhauer, and J. Sirker, Slow delocalization of particles in many-body localized phases, Phys. Rev. B **103**, 024203 (2021).
[53] T. LeBlond, D. Sels, A. Polkovnikov, and M. Rigol, Universality in the onset of quantum chaos in many-body systems, Phys. Rev. B **104**, L201117 (2021).
[54] D. Sels and A. Polkovnikov, Thermalization of dilute impurities in one dimensional spin chains, arXiv: 2105.09348.
[55] W. De Roeck and F. Huveneers, Stability and instability towards delocalization in many-body localization systems, Phys. Rev. B **95**, 155129 (2017).
[56] D. J. Luitz, F. Huveneers, and W. De Roeck, How a Small Quantum Bath can Thermalize Long Localized Chains, Phys. Rev. Lett. **119**, 150602 (2017).
[57] T. Thiery, F. Huveneers, M. Müller, and W. De Roeck, Many-Body Delocalization as a Quantum Avalanche, Phys. Rev. Lett. **121**, 140601 (2018).
[58] P. J. D. Crowley and A. Chandran, Avalanche induced coexisting localized and thermal regions in disordered chains, Phys. Rev. Res. **2**, 033262 (2020).
[59] D. Sels, Bath-induced delocalization in interacting disordered spin chains, Phys. Rev. B **106**, L020202 (2022).
[60] A. Morningstar, L. Colmenarez, V. Khemani, D. J. Luitz, and D. A. Huse, Avalanches and many-body resonances in many-body localized systems, Phys. Rev. B **105**, 174205 (2022).
[61] J.Šuntajs and L. Vidmar, Ergodicity Breaking Transition in Zero Dimensions, Phys. Rev. Lett. **129**, 060602 (2022).
[62] P. J. D. Crowley and A. Chandran, Mean field theory of failed thermalizing avalanches, Phys. Rev. B **106**, 184208 (2022).

[63] R. K. Panda, A. Scardicchio, M. Schulz, S. R. Taylor, and M. Žnidarič, Can we study the many-body localisation transition?, Europhys. Lett. **128**, 67003 (2020).
[64] P. Sierant, D. Delande, and J. Zakrzewski, Thouless Time Analysis of Anderson and Many-Body Localization Transitions, Phys. Rev. Lett. **124**, 186601 (2020).
[65] P. Sierant, M. Lewenstein, and J. Zakrzewski, Polynomially Filtered Exact Diagonalization Approach to Many-Body Localization, Phys. Rev. Lett. **125**, 156601 (2020).
[66] D. Abanin, J. Bardarson, G. De Tomasi, S. Gopalakrishnan, V. Khemani, S. Parameswaran, F. Pollmann, A. Potter, M. Serbyn, and R. Vasseur, Distinguishing localization from chaos: Challenges in finite-size systems, Ann. Phys. (Amsterdam) **427**, 168415 (2021).
[67] Á. L. Corps, R. A. Molina, and A. Relaño, Signatures of a critical point in the many-body localization transition, SciPost Phys. **10**, 107 (2021).
[68] A. Prakash, J. H. Pixley, and M. Kulkarni, Universal spectral form factor for many-body localization, Phys. Rev. Res. **3**, L012019 (2021).
[69] J. Schliemann, J. V. I. Costa, P. Wenk, and J. C. Egues, Many-body localization: Transitions in spin models, Phys. Rev. B **103**, 174203 (2021).
[70] M. Hopjan, G. Orso, and F. Heidrich-Meisner, Detecting delocalization-localization transitions from full density distributions, Phys. Rev. B **104**, 235112 (2021).
[71] A. Solórzano, L. F. Santos, and E. J. Torres-Herrera, Multifractality and self-averaging at the many-body localization transition, Phys. Rev. Res. **3**, L032030 (2021).
[72] G. De Tomasi, I. M. Khaymovich, F. Pollmann, and S. Warzel, Rare thermal bubbles at the many-body localization transition from the Fock space point of view, Phys. Rev. B **104**, 024202 (2021).
[73] P. J. D. Crowley and A. Chandran, A constructive theory of the numerically accessible many-body localized to thermal crossover, SciPost Phys. **12**, 201 (2022).
[74] R. Ghosh and M. Žnidarič, Resonance-induced growth of number entropy in strongly disordered systems, Phys. Rev. B **105**, 144203 (2022).
[75] N. Bölter and S. Kehrein, Scrambling and many-body localization in the XXZ chain, Phys. Rev. B **105**, 104202 (2022).
[76] Y. Zhang and Y. Liang, Optimizing randomized potentials for inhibiting thermalization in one-dimensional systems, Phys. Rev. Res. **4**, 023091 (2022).
[77] P. Sierant and J. Zakrzewski, Challenges to observation of many-body localization, Phys. Rev. B **105**, 224203 (2022).
[78] J. Sutradhar, S. Ghosh, S. Roy, D. E. Logan, S. Mukerjee, and S. Banerjee, Scaling of the Fock-space propagator and multifractality across the many-body localization transition, Phys. Rev. B **106**, 054203 (2022).
[79] F. B. Trigueros and C.-J. Lin, Krylov complexity of many-body localization: Operator localization in Krylov basis, SciPost Phys. **13**, 037 (2022).
[80] D. Z. Shi, V. Khemani, R. Vasseur, and S. Gopalakrishnan, Many body localization transition with correlated disorder, Phys. Rev. B **106**, 144201 (2022).
[81] J. M. Deutsch, Quantum statistical mechanics in a closed system, Phys. Rev. A **43**, 2046 (1991).
[82] M. Srednicki, Chaos and quantum thermalization, Phys. Rev. E **50**, 888 (1994).
[83] M. Rigol, V. Dunjko, and M. Olshanii, Thermalization and its mechanism for generic isolated quantum systems, Nature (London) **452**, 854 (2008).
[84] L. D'Alessio, Y. Kafri, A. Polkovnikov, and M. Rigol, From quantum chaos and eigenstate thermalization to statistical mechanics and thermodynamics, Adv. Phys. **65**, 239 (2016).
[85] See Supplemental Material at http://link.aps.org/supplemental/10.1103/PhysRevLett.129.260601 for reorthogonalization of LIOMs in the subspace with fixed number of fermions, absence of projection of H_Δ on LIOMs, derivation of Eq. (7) and the lower bound on the norm of the true perturbation, the details about the nearest level spacing analysis and the fluctuations of the diagonal matrix elements.
[86] In contrast, in translationally invariant integrable models the products of local charges are typically nonlocal thus, in the thermodynamic limit, they have no projection on local observables.
[87] Y. Y. Atas, E. Bogomolny, O. Giraud, and G. Roux, Distribution of the Ratio of Consecutive Level Spacings in Random Matrix Ensembles, Phys. Rev. Lett. **110**, 084101 (2013).
[88] M. Fremling, Exact gap-ratio results for mixed Wigner surmises of up to 4 eigenvalues, arXiv:2202.01090.
[89] O. Giraud, N. Macé, E. Vernier, and F. Alet, Probing Symmetries of Quantum Many-Body Systems through Gap Ratio Statistics, Phys. Rev. X **12**, 011006 (2022).
[90] M. Schreiber, S. S. Hodgman, P. Bordia, H. P. Lüschen, M. H. Fischer, R. Vosk, E. Altman, U. Schneider, and I. Bloch, Observation of many-body localization of interacting fermions in a quasi-random optical lattice, Science **349**, 842 (2015).
[91] H. Kim, T. N. Ikeda, and D. A. Huse, Testing whether all eigenstates obey the eigenstate thermalization hypothesis, Phys. Rev. E **90**, 052105 (2014).
[92] R. Mondaini, K. R. Fratus, M. Srednicki, and M. Rigol, Eigenstate thermalization in the two-dimensional transverse field Ising model, Phys. Rev. E **93**, 032104 (2016).
[93] D. Jansen, J. Stolpp, L. Vidmar, and F. Heidrich-Meisner, Eigenstate thermalization and quantum chaos in the Holstein polaron model, Phys. Rev. B **99**, 155130 (2019).
[94] S. Iyer, V. Oganesyan, G. Refael, and D. A. Huse, Many-body localization in a quasiperiodic system, Phys. Rev. B **87**, 134202 (2013).
[95] M. Schulz, C. A. Hooley, R. Moessner, and F. Pollmann, Stark Many-Body Localization, Phys. Rev. Lett. **122**, 040606 (2019).
[96] E. van Nieuwenburg, Y. Baum, and G. Refael, From Bloch oscillations to many-body localization in clean interacting systems, Proc. Natl. Acad. Sci. U.S.A. **116**, 9269 (2019).